Solid-State Electronics 200 (2023) 108509

Contents lists available at ScienceDirect

Solid State Electronics

journal homepage: www.elsevier.com/locate/sse

Theoretical study of carrier transport in supported and gated two-dimensional transition metal dichalcogenides☆

Sanjay Gopalan [a,*], Maarten L. Van de Put [b], Gautam Gaddemane [b], Massimo V. Fischetti [a]

[a] The University of Texas at Dallas, 800 West Campbell Road, Richardson 75080, TX, USA
[b] imec, Kapeldreef 75, B-3001 Leuven, Belgium

ARTICLE INFO

The review of this paper was arranged by "Francisco Gamiz"

Keywords:
Transport
Monte-Carlo
DFT
TMD
Mobility
Dielectric
Theoretical
2D

ABSTRACT

We investigate theoretically the impact of the dielectric environment on electronic transport in transition metal dichalcogenide monolayers. The low-field carrier mobility in free-standing layers is calculated using well-known *ab initio* methods, and the study is extended to layers in double-gate structures using the dielectric continuum approximation. In particular, we account for the screening of the electron–phonon interaction by the free carriers in the layer and by the dielectric environment. In addition, we include scattering with the hybrid interface optical-phonon/plasmon excitations ("remote phonons"). We find that whereas the presence of insulators with a high dielectric constant may increase the carrier mobility when ignoring the latter process, scattering with the hybrid interface excitations negates this beneficial effects and depresses the mobility significantly below its value in free-standing monolayers.

1. Introduction

Theoretical methods are critical for evaluating two-dimensional materials as possible channel materials in future field-effect transistors (FETs). The majority of modeling attempts concentrate on electronic transport in ideal free-standing layers, ignoring the dielectric environment's effect on the transport characteristics. Although, few studies have been reported on the effects of the dielectric environment on two-dimensional (2D) materials [1,2], these studies have been based on simplifications of the problem, for example by ignoring the full hybridization of all phonon-like and plasmon-like modes or the effects of free-carrier screening, or by using approximate dispersions of the hybrid modes. In this work, we study the scattering of electrons with the coupled (hybrid) optical-phonon/plasmon excitations that are present at the interfaces double-gated structures consisting of a polar 2D semiconductor (a TMD) with top and bottom gate insulators and ideal-metal gate contacts. However, of particular interest is the work done by Hauber and Fahy [3]. They present a careful analysis of the plasmon/optical-phonon excitations in bulk III-V compound semiconductors and supported and gated thin MoS_2 layers. However, they have considered only a limited set of gate insulators and the TMDs. We perform an extensive study of the electron mobility in supported and/or gated monolayer TMDs in the presence of hybrid interface optical-phonon/plasmon (IPP) excitations, extending the study of the room-temperature electron mobility not only in MoS_2 but also in WS_2, $MoTe_2$, and of the 300 K hole mobility in WSe_2 and WTe_2, with all TMDs assumed to be supported by SiO_2 and with SiO_2, HfO_2, Al_2O_3, AlN, and hBN as gate insulators with an equivalent oxide thickness of 0.7 nm.

2. Theory

The system we consider, shown in Fig. 1, consists of an ideal (bottom) metal gate in the region $z \leqslant -t_b$; an insulator (which can be viewed either as a substrate, when $t_b \to \infty$, or as a bottom gate insulator) with dielectric function $\epsilon_{box}(\omega)$ in the region $-t_b < z \leqslant 0$; a 2D layer of thickness h and dielectric function $\epsilon_{2D}(Q,\omega)$ in the region $0 < z \leqslant h$; a gate insulator with dielectric function $\epsilon_{tox}(\omega)$ in the region $h < z \leqslant h + t_t$; and an ideal metal in the half-space $z > h + t_t$. With regards to notation in this paper, we use the lower-case bold symbols (such as **r** or **k**) to deNote 3-vectors and uppercase bold symbols (such as **R** or **K**) to deNote

☆ This work has been funded by the Semiconductor Research Corporation (SRC) nCORE/NEWLIMITS program and, in part, by the Taiwan Semiconductor Manufacturing Company Ltd. (TSMC).

* Corresponding author.
E-mail address: sanjay.gopalan@utdallas.edu (S. Gopalan).

https://doi.org/10.1016/j.sse.2022.108509
Received 5 July 2022; Received in revised form 20 October 2022; Accepted 23 October 2022
Available online 30 October 2022
0038-1101/© 2022 Elsevier Ltd. All rights reserved.

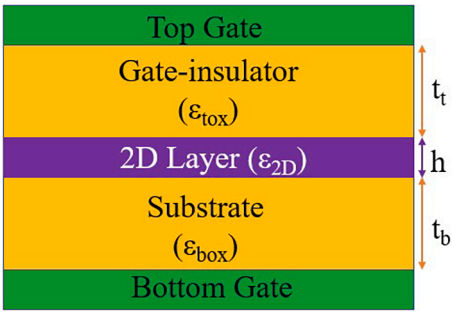

Fig. 1. The double-gated TMD monolayer.

2-vectors on the (x, y) plane of the layer.

2.1. Screening of electron–phonon interaction

In order to consider how the dielectric environment may affect the carrier-phonon scattering rates calculated using DFT, we note the matrix elements associated with these processes have the form:

$$\langle \mathbf{K}'|\delta E^{(\eta)}_{\rm tot}|\mathbf{K}\rangle = \int {\rm d}\mathbf{r}\ \psi^{*}_{\mathbf{K}'}(\mathbf{r})\ \delta E^{(\eta)}_{\rm tot}(\mathbf{r})\ \psi_{\mathbf{K}}(\mathbf{r}), \tag{1}$$

where $\psi_{\mathbf{K}}(\mathbf{r})$ is the Bloch wave of electrons with wave vector $\mathbf{K}$ in the TMD layer (having omitted for simplicity the band index) and $\delta E^{(\eta)}_{\rm tot}(\mathbf{r})$ is the change of the total energy of the system caused by a phonon of branch η. Both the Hartree and the exchange–correlation potentials contribute to this change; that is, $\delta E^{(\eta)}_{tot}(\mathbf{r}) = \delta E^{(\eta)}_{\rm H}(\mathbf{r}) + \delta E^{(\eta)}_{\rm xc}(\mathbf{r})$. Since the Hartree energy, $E_{\rm H}(\mathbf{r})$, depends linearly on the electron density, whereas $E_{\rm xc}(\mathbf{r})$ has a weaker dependence (namely $E_{\rm xc}(\mathbf{r}) \sim \rho^{(\eta)}(\mathbf{r})^{1/3}$ in the local-density approximation, LDA), we consider only the change of the Hartree component:

$$\delta E_{\rm tot}(\mathbf{r}) \approx \delta E^{(\eta)}_{\rm H}(\mathbf{r}) = \int d\mathbf{r}'\ G^{(0)}(\mathbf{r},\mathbf{r}')\,\delta\rho^{(\eta)}(\mathbf{r}'), \tag{2}$$

where $G^{(0)}(\mathbf{r},\mathbf{r}')$ is the Green's function for the Poisson equation *in vacuo* and $\delta\rho^{(\eta)}(\mathbf{r}')$ is the change of the charge at $\mathbf{r}'$ induced by the phonon. This can be expressed as:

$$\delta\rho^{(\eta)}(\mathbf{r}') = \sum_{al} \widetilde{\nabla}_{\mathbf{R}_{al}}\,\delta\rho(\mathbf{r}')\cdot\delta\mathbf{R}^{(\eta)}_{al} \tag{3}$$

where the quantity $\delta\mathbf{R}^{(\eta)}_{al}$ is the displacement of the ion α in cell l due to phonons of branch η. The symbol $\widetilde{\nabla}$ denotes the 'functional gradient', so that the quantity $\widetilde{\nabla}_{\mathbf{R}_{al}}\,\delta\rho(\mathbf{r}')$ represents the change of the electronic charge ρ at position $\mathbf{r}'$ under an infinitesimal shift of ion α in cell l along the Cartesian directions. Thus, writing the 'final' electronic state $\mathbf{K}'$ in terms of the phonon wave vector $\mathbf{Q}$ as $\mathbf{K}' = \mathbf{K} + \mathbf{Q}$, the electron–phonon matrix element can be written as:

$$\langle \mathbf{K}+\mathbf{Q}|\delta E^{(\eta)}_{\rm H}|\mathbf{K}\rangle = \sum_{\mathbf{g}\mathbf{g}'} u^{*}_{\mathbf{K}+\mathbf{Q},\mathbf{g}'}\ u_{\mathbf{K},\mathbf{g}} \sum_{\alpha} e^{-i\mathbf{Q}\cdot\tau_\alpha} \times A^{(\eta,\alpha)}_{\mathbf{Q}}\,\mathbf{e}^{(\eta,\alpha)}_{\mathbf{Q}}\cdot\nabla_{\tau_\alpha}\rho_{\mathbf{Q}}\,G^{(\rm vac)}_{\mathbf{Q}}(d,d), \tag{4}$$

where $A^{(\eta,\alpha)}_{\mathbf{Q}}$ is a quantity whose square is proportional to the ionic displacement and to the Bose–Einstein coefficients, $d = h/2$ is the 'vertical' coordinate in the middle of the layer, and $G^{(\rm vac)}_{\mathbf{Q}}(z,z')$ is the 2D Fourier transform of the Poisson Green's function (that is: the potential at z due to a point charge at z') of a system consisting of a 2D layer of dielectric constant ϵ^{∞}_{2D} and thickness h. We now use Eqs. (1)–(3), the method followed in Ref. [4] and assume that: **i)** that the change of total energy of the system in Eq. 1 is dominated by the Hartree component; **ii)** that only the in-plane ionic displacement are considered; **iii)** that the charge response to the ionic motion is localized at $z' = d = h/2$; **iv)** that the Poisson Green's function is constant over the effective thickness (h) of the 2D layer; **v)** that *Umklapp* processes may be ignored, since the Poisson Green's function decays quickly as Q increases, Thus, we can account for the effects of the dielectric environment by simply replacing the 'vacuum' Poisson Green's function $G^{(\rm vac)}_{Q}(d,d)$ with the Green's function for Poisson equation $G^{(\rm env)}_{Q,\omega^{(\eta)}_{Q}}(d,d)$ with the boundary conditions dictated by the double-gate geometry described earlier in this section (Fig. 1). For a given scattering process involving a phonon of branch η and wave vector $\mathbf{Q}$, we can account for the presence of the different dielectric environment and free-carrier screening by simply rescaling the scattering rates calculated using DFT/EPW by the squared ratio:

$$\left|\frac{\mathscr{G}^{(env)}_{Q,\omega^{(\eta)}_{Q}}(d,d)}{\mathscr{G}^{(\rm vac)}_{Q}(d,d)}\right|^2 \tag{5}$$

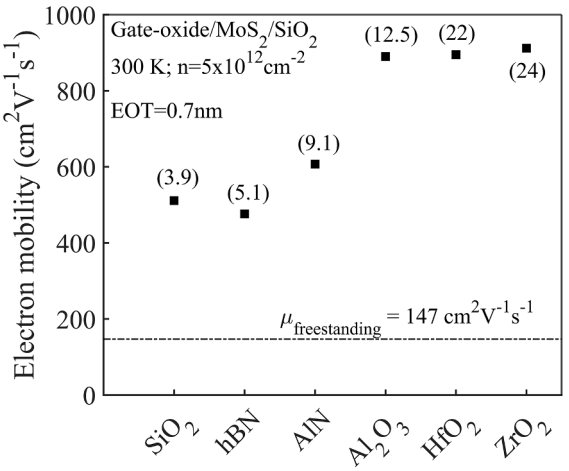

Fig. 2. Calculated 300 K electron mobility in the TMD channel of a gate-insulator/MoS_2/SiO_2 structure including only the effect of free-carrier and dielectric screening by the dielectrics (ordered with increasing static dielectric constant – shown in parentheses –from left to right).

2.2. Electron-IPP scattering

When introducing polar substrates and gate-insulators, we have to consider the interaction of coupled interface-plasmon phonon (IPP) modes with the charge carriers in the channel. The scattering potential is given by the usual Fröhlich-like term [5]. This evaluation requires the calculation of the dispersion of the hybrid IPP modes [6,7]. Since the complete theory is too elaborate to present here, we refer to the Refs. [5–7] for a complete discussion. The scattering amplitude $\mathscr{A}^{(\alpha)}_{Q,\omega^{(i)}_{Q}}$ of the potential due to the α-phonon-content $\Phi^{(\alpha)}(\omega^{(i)}_{Q})$ of the hybrid mode i is given by:

$$|\mathscr{A}^{(\alpha)}_{Q,\omega^{(i)}_{Q}}|^2 = \Phi^{(\alpha)}(\omega^{(i)}_{Q})\left(1-e^{-2Qt_{\rm b}}\right)^2 \frac{e^2\hbar\omega^{(i)}_{Q}}{2Q}\left|\frac{1}{\epsilon^{(\alpha,\rm high)}_{\rm TOT}(Q,\omega^{(i)}_{Q})} - \frac{1}{\epsilon^{(\alpha,\rm low)}_{\rm TOT}(Q,\omega^{(i)}_{Q})}\right| \tag{6}$$

The 'total' dielectric function $\epsilon_{\rm TOT}(Q,\omega)$ is given by a rather complicated expression appearing at the right-hand side of the secular equation whose solutions give the dispersion of the IPPs. The superscripts 'high' and 'low' indicate that the function has to be calculated assuming the bare phonon α does not respond or responds fully, respectively.

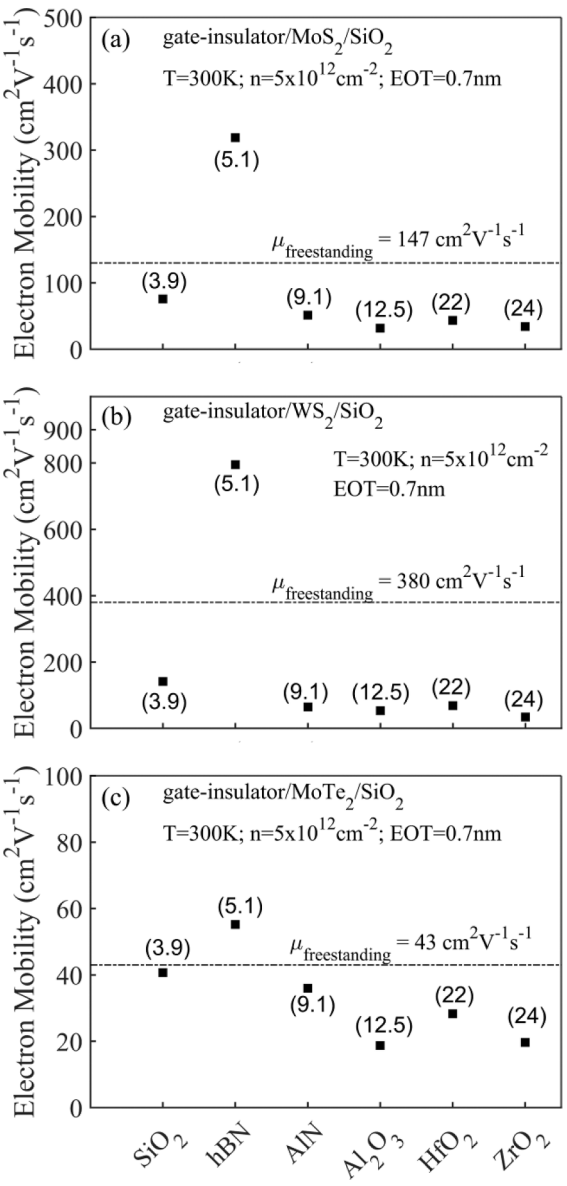

Fig. 3. (a): Calculated 300 K electron mobility in the TMD channel of a SiO_2/MoS_2/gate-insulator structure with different gate-insulators (ordered with increasing static dielectric constant – shown in parentheses – from left to right). (b): The same, but for the SiO_2/WS_2/gate-insulator structure and (c), for the SiO_2/$MoTe_2$/gate-insulator structure.

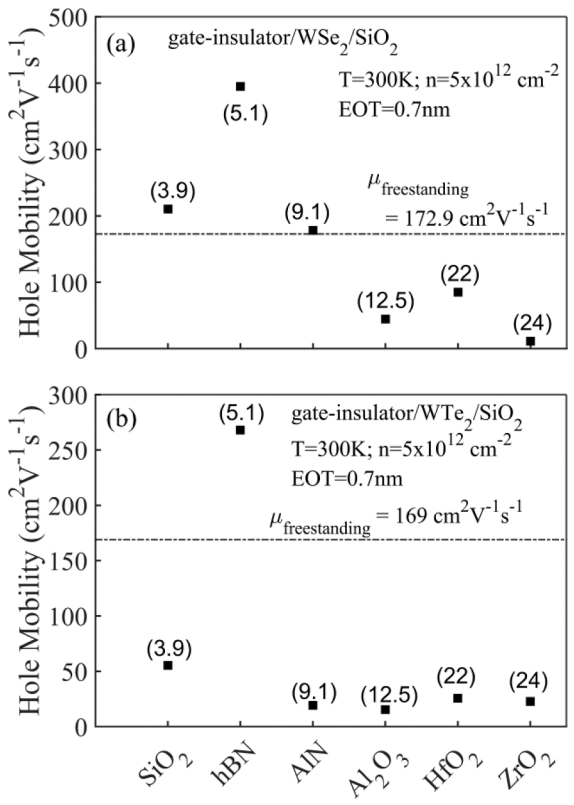

Fig. 4. (a): Calculated 300 K hole mobility in the TMD channel of a SiO_2/WSe_2/gate-insulator structure with different gate-insulators (ordered with increasing static dielectric constant – shown in parentheses – from left to right). (b): The same, but for the SiO_2/WTe_2/gate-insulator structure.

3. Results

We have calculated the low-field carrier mobility in the TMD channel of the double-gate system shown in Fig. 1 using the full-band Monte Carlo procedure described in Refs. [8–10]. In this study, we have used the GGA-PBE approximation [11] for the exchange–correlational functionals and the Optimized Norm-Conserving Vanderbilt pseudopotentials [12] and the electronic band structure, phonon dispersion and free-standing electron–phonon matrix elements have been reported in Ref. [10]. The dielectric constant and layer thickness of the TMDs have been obtained from Ref. [13].

Fig. 2 shows the effect of only free-carrier and dielectric screening on the mobility of the double-gated gate-insulator/MoS_2/SiO_2 system. For reference, the electron mobility of a free-standing MoS_2 layer, without screening is 147 $cm^2V^{-1}s^{-1}$ [10]. As expected, the mobility increase with increasing dielectric constant of the substrate, with higher dielectric constant providing stronger screening of the electron–phonon interactions. Screening by the highest-κ dielectrics we consider, HfO_2 and ZrO_2, increases the phonon-limited electron mobility of MoS_2 by almost one order of magnitude (> 900 $cm^2V^{-1}s^{-1}$). Even in the case of SiO_2, one can see some modest gains, with an electron mobility of about 500 $cm^2V^{-1}s^{-1}$. A similar beneficial effect of the screening induced by high-κ dielectrics has been observed [14,15] and theoretically explained [16] in the case of the impurity-limited mobility of MoS_2.

While these results may seem promising, Figs. 3 and 4 shows that, once the interaction with the IPP modes are considered, the carrier mobility of double-gated 2D-TMDs is degraded well below the free-standing mobility, in most cases of gate-insulator considered. Among the various supported and gated TMDs considered, the best electron mobility, 795 $cm^2V^{-1}s^{-1}$, is obtained for the SiO_2/WS_2/hBN system. An excellent hole mobility, 396 $cm^2V^{-1}s^{-1}$ is also predicted for the SiO_2/WSe_2/hBN. These extended results confirm the general trend observed previously for MoS_2 [17]: The carrier mobility decreases almost monotonically with increasing dielectric constant of the gate insulator, with two exceptions: 1. The beneficial effects of dielectric screening of the 'out-of-plane' field lines are seen for hBN, thanks to its relatively low ionic polarization and the high phonon frequencies resulting from the light weight of the B and N ions. 2. On the contrary, resonance effects among the optical phonons of the substrate, of the TMD layer, and of the gate-insulator result in a low carrier mobility when AlN and/or Al_2O_3 are taken as gate insulators. The resonance effect has been already predicted theoretically for the Si/SiO_2/poly-Si-gate system. When the poly-Si density yields a plasma frequency close to the TO-frequency of SiO_2, the resonance of these two modes causes a low carrier mobility (Ref. [18]). Fig. 3 shows the electron mobility results for various combinations. Looking at the Fig. 3(a), one notices that the calculated 300 K electron mobility in SiO_2-supported monolayer MoS_2 decreases as the gate insulator is changed from hBN to HfO_2, but it reaches a particularly

high value for hBN and a very low value for Al_2O_3. A similar behavior is seen also for the 300 K electron mobility of WS_2 (Fig. 3)) and $MoTe_2$ (Fig. 3(c)), when AlN is taken as gate insulator. We observe a similar trend in the 300 K hole mobility of WSe_2 (Fig. 4)) and WTe_2 (Fig. 4(b)). In all cases, hBN exhibits the best mobility, even higher than in free-standing monolayers, thanks to the dielectric screening of the out-of-layer field lines and the weak remote-phonon scattering due to its weak polar nature and light ions (resulting in high phonon frequencies, decoupled from all other excitations).

4. Conclusion

We have studied theoretically how the dielectric environment affects low-field electronic transport in two-dimensional transition metal dichalcogenides. The carrier mobility improves significantly when considering only the effect of dielectric screening by the free carriers and the surrounding dielectrics. However, these positive effects are countered by the detrimental effects due to the electron-IPP interaction. The carrier mobility decreases significantly below its value in free-standing monolayers with increasing dielectric constant of the insulator(s). 'Phonon resonance' occurs when two optical phonons of the dielectrics have similar frequencies and it results in an even stronger depression of the mobility. Moreover, the weak ionic polarizability of hBN results in the highest carrier mobility, although the relatively low dielectric constant of hBN negates the scaling benefits of high-κ insulators. Nonetheless, in most cases, the transport properties of TMDs remain disappointing. However, some combination of gate-insulator and the substrate may give competitive transport properties when compared to well-known ultra-thin Si system.

Declaration of Competing Interest

Sanjay Gopalan reports financial support was provided by Semiconductor Research Corp. Sanjay Gopalan reports financial support was provided by Taiwan Semiconductor Manufacturing Co Ltd.

References

[1] Zeng L, Xin Z, Chen S, Du G, Kang J, Liu X. Remote phonon and impurity screening effect of substrate and gate dielectric on electron dynamics in single layer MoS_2. Appl Phys Lett 2013;103:113505 .

[2] Ma N, Jena D. Charge scattering and mobility in atomically thin semiconductors. Phys Rev X 2014;4:011043 .

[3] Hauber A, Fahy S. Scattering of carriers by coupled plasmon-phonon modes in bulk polar semiconductors and polar semiconductor heterostructures. Phys Rev B 2017; 95:045210 .

[4] Gopalan S, Van de Put ML, Gaddemane G, Fischetti MV, Theoretical study of electronic transport in two-dimensional transition metal dichalcogenides: Effects of the dielectric environment, arXiv preprint arXiv:2208.11031 (2022).

[5] Fischetti MV, Neumayer DA, Cartier EA. Effective electron mobility in Si inversion layers in metal–oxide–semiconductor systems with a high-κ) insulator: The role of remote phonon scattering. J Appl Phys 2001;90:4587–608.

[6] Ong Z-Y, Fischetti MV. Theory of remote phonon scattering in top-gated single-layer graphene. Phys Rev B 2013;88:045405 .

[7] Ong Z-Y, Fischetti MV. Theory of interfacial plasmon-phonon scattering in supported graphene. Phys Rev B 2012;86:165422 .

[8] Gaddemane G, Vandenberghe WG, Van de Put ML, Chen S, Tiwari S, Chen E, Fischetti MV. Theoretical studies of electronic transport in monolayer and bilayer phosphorene: A critical overview. Phys Rev B 2018;98:115416 .

[9] Gaddemane G, Vandenberghe WG, Van de Put ML, Chen E, Fischetti MV. Monte-Carlo study of electronic transport in non-σ_h-symmetric two-dimensional materials: Silicene and germanene. J Appl Phys 2018;124:044306 .

[10] Gaddemane G, Gopalan S, Van de Put ML, Fischetti MV. Limitations of ab initio methods to predict the electronic-transport properties of two-dimensional semiconductors: the computational example of 2H-phase transition metal dichalcogenides. J Comput Electron 2021;20:49–59.

[11] Perdew JP, Burke K, Ernzerhof M. Generalized gradient approximation made simple. Phys Rev Lett 1996;77:3865.

[12] Hamann D. Optimized norm-conserving Vanderbilt pseudopotentials. Phys Rev B 2013;88:085117 .

[13] Laturia A, Van de Put ML, Vandenberghe WG. Dielectric properties of hBN and transition metal dichalcogenides: from monolayer to bulk, npj 2D. Mater Appl 2018;2:1–7.

[14] Radisavljevic B, Radenovic A, Brivio J, Giacometti V, Kis A. Single-layer MoS_2 transistors. Nat Nanotech 2011;6:147.

[15] Radisavljevic B, Kis A. Mobility engineering and metal-insulator transition in monolayer MoS_2. Nat Mater 2013;12:815.

[16] Ong Z-Y, Fischetti MV. Mobility enhancement and temperature dependence in top-gated single-layer MoS_2. Phys Rev B 2013;88:165316 .

[17] Van de Put ML, Gaddemane G, Gopalan S, Fischetti MV, Effects of the Dielectric Environment on Electronic Transport in Monolayer MoS_2: Screening and Remote Phonon Scattering, in: 2020 International Conference on Simulation of Semiconductor Processes and Devices (SISPAD 2020, IEEE, 2020, pp. 281–284.

[18] Kotlyar R, Giles M, Matagne P, Obradovic B, Shifren L, Stettler M, Wang E, Inversion mobility and gate leakage in high-k/metal gate MOSFETs, in: IEDM Technical Digest, 2004, IEEE, 2004, pp. 391–394.